Transactions on Engineering Sciences vol 43, © 2003 WIT Press, www.witpress.com, ISSN 1743-3533

Experimental evaluation of wire mesh bearing dampers at cryogenic conditions

E. M. AL-Khateeb[1], B. H. Ertas[2], J. M. Vance[2]
[1]*Consulting Services Department, Saudi Aramco*
[2]*Mechanical Engineering Department, Texas A&M University*

Abstract

Mechanical and fluid dampers have been placed at bearing locations in turbomachinery to stabilize and attenuate vibration levels. Wire mesh, a material formed by compressing woven wires into the desired shape, possesses significant amounts of damping. As part of a broader effort to study the effects of different design factors, ring shaped wire mesh elements made of different materials and compression densities were tested to compound an understanding of how stiffness and damping behave in a cryogenic environment. The dynamic response to periodic excitations at cryogenic temperatures was compared to that of ambient conditions. Experimental results presented in this paper show the variation of stiffness and damping with temperature in addition to specific material dependent findings valuable for designing low temperature vibration dampers.

1 Introduction

Wire mesh possesses favourable attributes that make it a promising rotor vibration damper material for turbomachinery applications. In order to predict the performance of a wire mesh damper in turbomachinery applications, it is essential to identify its dynamic coefficients, basically stiffness and damping, and the different factors that could influence these coefficients. As part of an extensive investigation of the different factors affecting the behaviour of wire

mesh dampers [1], this research was conducted to study the performance of wire mesh at low (cryogenic) temperatures found in such applications as rocket or space shuttle engine turbopumps. Ring-shaped wire mesh elements, suitable for applications as bearing dampers, were used in the study. Figure 1 shows a typical wire mesh bearing damper element.

Significant amounts of damping from testing of wire mesh damper elements under adverse conditions have been reported by Al-Khateeb [1] and Zarzour and Vance [2]. Both series and parallel arrangements of the wire mesh element with the bearing have been laboratory tested in rotating test rigs by Zarzour and Vance [2] and Al-Khateeb [3], respectively. Ertas et al. [4] presented cryogenic test and rotordynamic analysis results for a wire mesh damper application in a liquid hydrogen turbopump [4]. Wire mesh dampers were also used to solve a rotordynamic instability problem in a rocket engine turbopump [5]. Furthermore, as part of a program to solve rotordynamic instability problems in the space shuttle main engine fuel turbopump, Childs [6] reported significant wire mesh damping measured in bench tests. Nonetheless, research to study wire mesh damper characteristics and behaviour under different conditions has been very scarce. The results presented in this paper aim to quantify thermal effects on the dynamic behaviour of wire mesh direct stiffness and damping coefficients. This should, at least, qualitatively guide designers of such a bearing damper for low temperature applications.

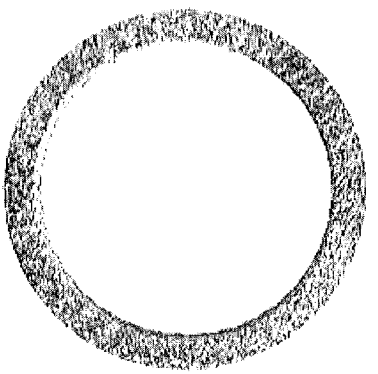

Figure 1: Wire Mesh Element.

2 Experimental apparatus

Experiments were performed using a cryogenic test rig, shown in Figure 2, to determine wire mesh stiffness and damping variation with temperature. Three of the six ring-shaped, compressed jersey-stitch wire mesh elements previously tested by Ertas et al. [4] were selected for these experiments. The three selected elements, numbered N2, N4 and N6, are representative of the previously tested densities and materials (high density steel, low density steel, and low density

copper wire meshes). Specifications of the tested wire mesh elements are given in Table 1. The test rig configuration consists basically of an insulated chamber casing with an integral journal on which the tested wire mesh element is fitted. A steel collar is fitted to the OD of the wire mesh element. Liquid nitrogen was used in the cryogenic tests to lower the wire mesh element's temperature, which was directly monitored with a suitable thermocouple.

An electromagnetic shaker was used to apply a dynamic force, measured by the force transducer, to the collar causing motion that is sensed by the proximity probe. Temperatures of measurement instrumentation were maintained within calibration ranges by using directed streams of heated air. The signals from the force transducer and proximity probe were collected and processed with a two-channel signal analyser.

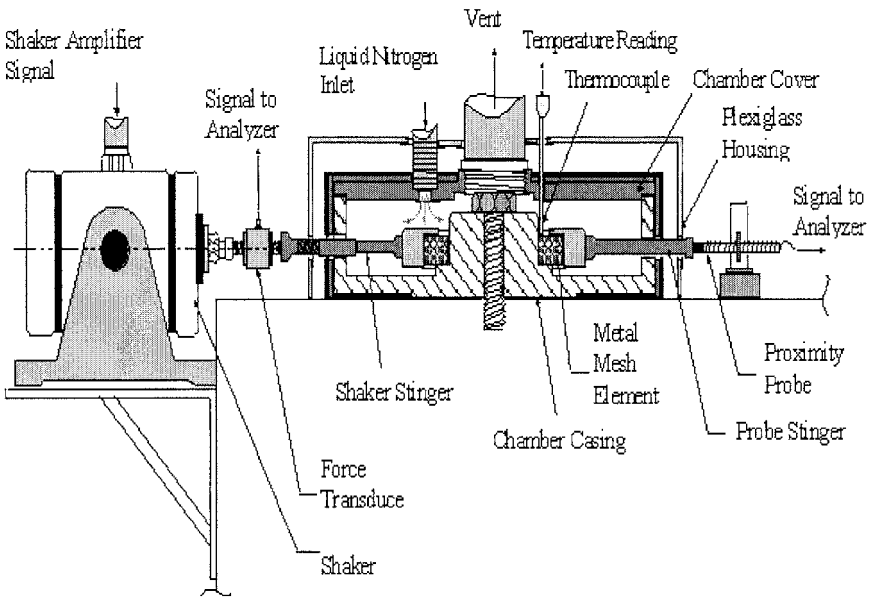

Figure 2: Cryogenic Test Rig.

Table 1: Physical Specifications for Wire Mesh Elements N1-N6.

Element Description		ID (mm)	OD (mm)	Thickness (mm)	Volume (cm^3)	Weight (N)	Density (%)
N2	**Steel - high density mesh**	68.580	94.437	10.897	36.074	1.1303	40.79%
N4	**Steel - low density mesh**	68.580	94.92	10.998	37.2	0.6187	21.65%
N6	**Copper - low density mesh**	68.580	93.167	10.668	33.321	0.7144	26.77%

3 Data collection and analysis

The data was obtained from sweeping-frequency sinusoidal excitation shaker tests on the test rig, which was designed as a single degree of freedom system in the testing frequency range. The instrumentation set-up is shown in Figure 3. The Dynamic Stiffness frequency response function data (amplitude, phase, real and imaginary parts, and coherence) in addition to raw waveforms were collected by the two-channel analyser having applied force and resulting displacement as inputs. Frequency domain parameter identification methods [1] were used for extracting the stiffness and damping coefficient values from test data. The maximum displacement amplitude was maintained the same in different tests in order to exclude the effect of amplitude dependency [1].

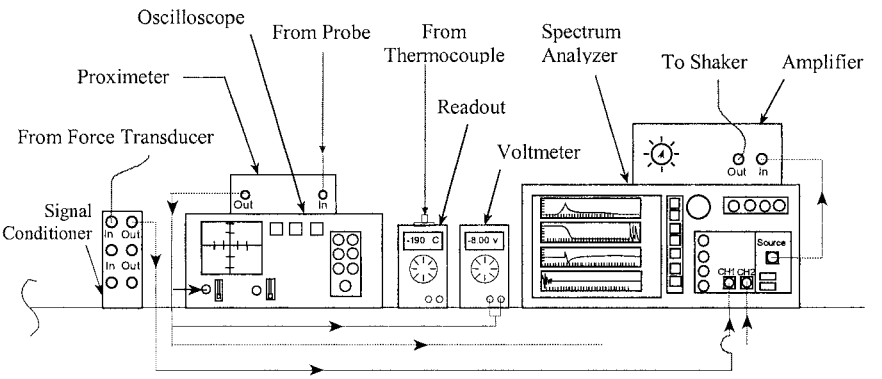

Figure 3: Instrumentation Set-up Diagram.

4 Experimental results

In earlier experiments by Ertas et al. [4], the wire mesh elements were tested at two temperatures; ambient and cryogenic. Figures 4 through 7 show typical plots of test data from those experiments. Table 2 compares ambient and cryogenic values of the wire mesh elements' stiffness and damping coefficients from the experiments by Ertas et al. [4]. These results intrinsically include the effects of both temperature and change of external stresses (interference fit), due to material shrinkage, on the tested wire mesh element. The results presented in this paper extend earlier efforts by testing the three wire mesh elements at several temperatures, from ambient to cryogenic, and excluding the effects of changing interference fit with temperature. This helps to better understand and isolate wire mesh behaviour with temperature.

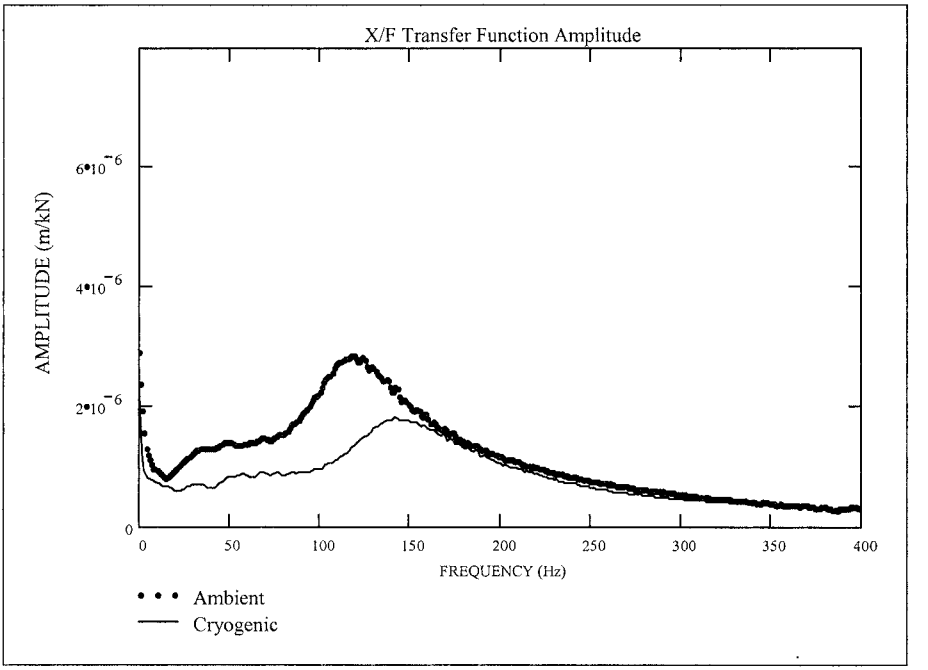

Figure 4: Typical Temperature Effects on X/F Transfer Function Magnitude [4].

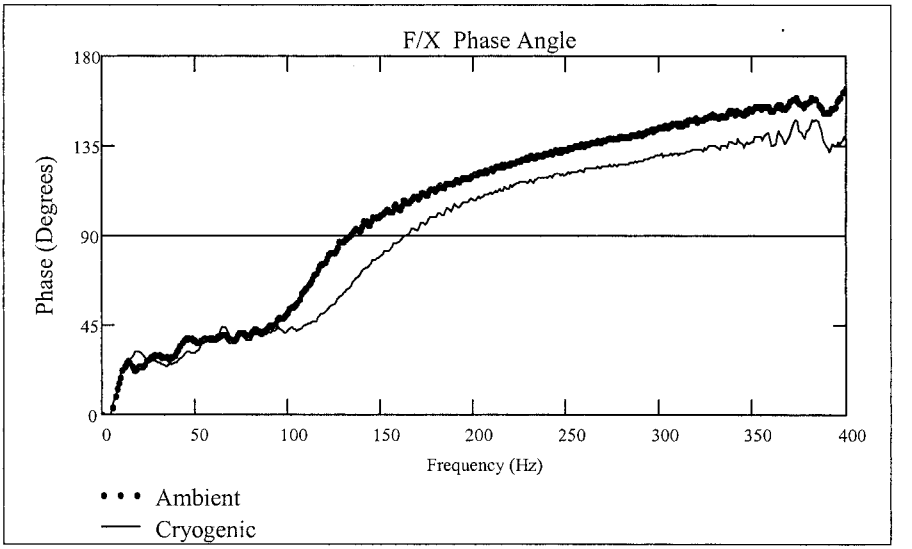

Figure 5: Typical Temperature Effects on Transfer Function Phase.

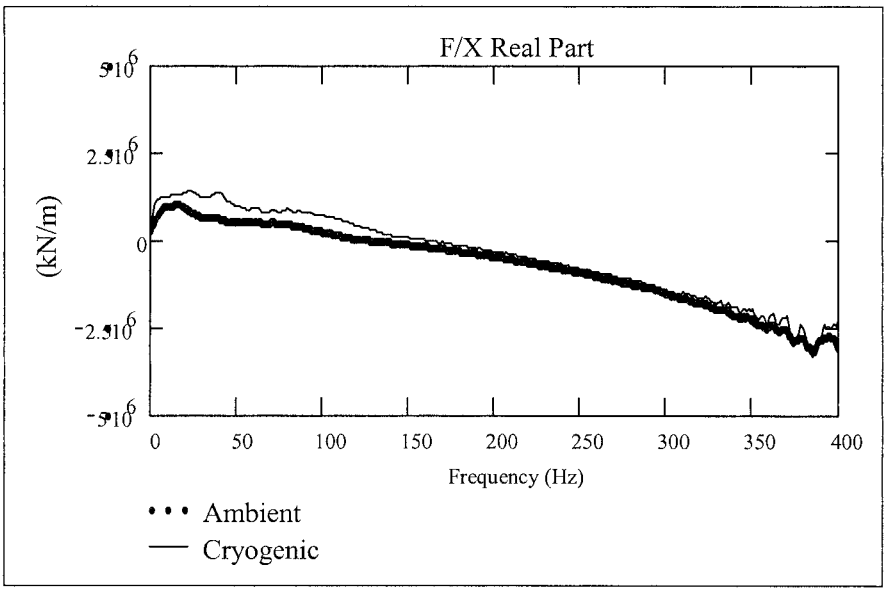

Figure 6: Typical Temperature Effects on Transfer Function Real Part.

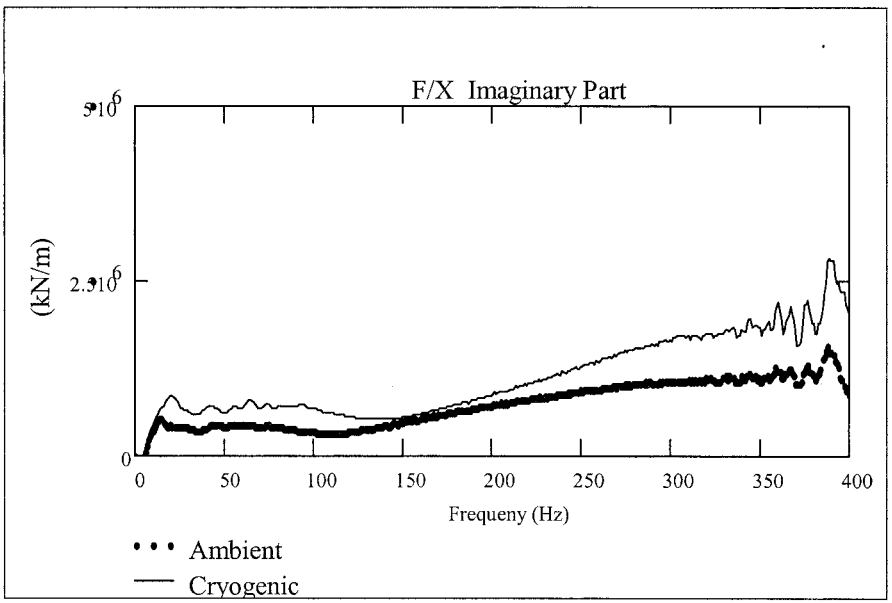

Figure 7: Typical Temperature Effects on Transfer Function Imaginary Part.

Table 2: Cryogenic / Ambient Test Results [4].

	Ambient				Cryogenic				Percentage Change		
Wire Mesh	Fit mm	K kN/m	C N-s/m	H kN/m	T °C	K kN/m	C N-s/m	H kN/m	ΔK %	ΔC %	ΔH %
N2	0.051	1189	528.2	544	-175	1676	506.1	584	41	-4	7
N3	0.381	1487	645.0	783	-170	3203	669	1094	115	4	40
N4	0.279	1452	659.6	806	-165	3144	584.3	967	116	-11	20
N5	0.432	663	463.5	373	-180	994	592.5	586	50	28	57
N6	0.305	741	491.5	419	-155	1184	619.3	627	60	26	50
N6 Hi Fit	0.559	1434	594.2	686	-190	2226	811.4	1170	55	36	70

Significant material shrinkage occurs due to low temperatures resulting in a change of the interference fit applied to the tested wire mesh element. Therefore, correlations between interference and wire mesh stiffness and damping by Al-Khateeb [1] were used to exclude the effects of interference. The maximum displacement amplitudes during the tests were kept at 0.152 mm (6 mils) ±15%, peak to peak. If other conditions remain the same, a lower displacement amplitude should result in higher damping and stiffness [1].

Results from experiments on wire mesh elements N2, N4 and N6 are given below. Plots of the extracted wire mesh stiffness and damping (viscous and hysteretic) coefficients before and after subtracting the contribution of interference are shown in Figures 8 through 10. Figure 11 is a plot of the loss coefficient (β) calculated by dividing the hysteretic damping coefficient (H) by the stiffness coefficient (K):

$$\beta = H/K \tag{1}$$

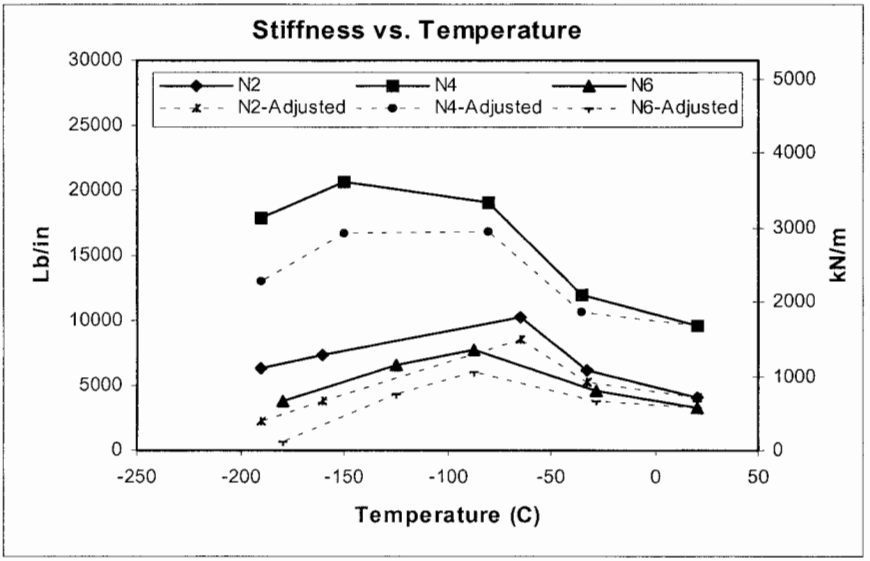

Figure 8: Wire Mesh Stiffness Coefficients before and after Subtracting Interference Fit Contribution.

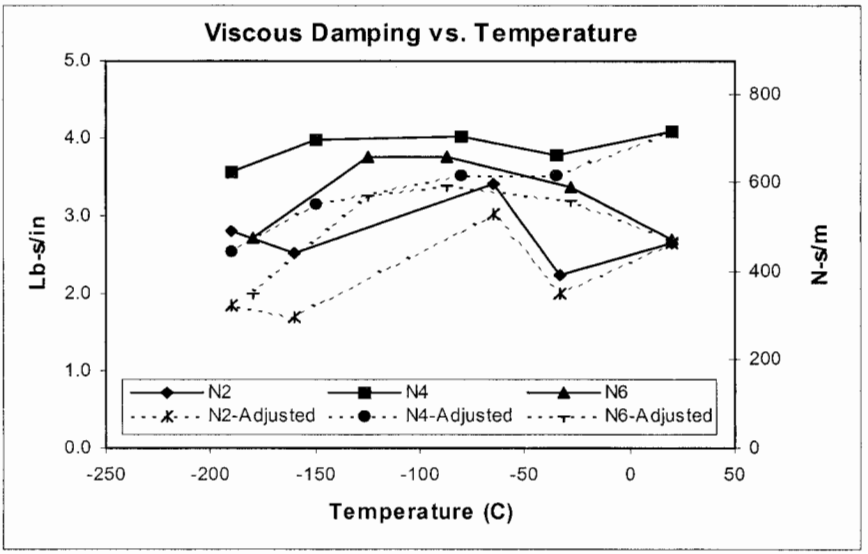

Figure 9: Viscous Damping Coefficients before and after Subtracting Interference Fit Contribution.

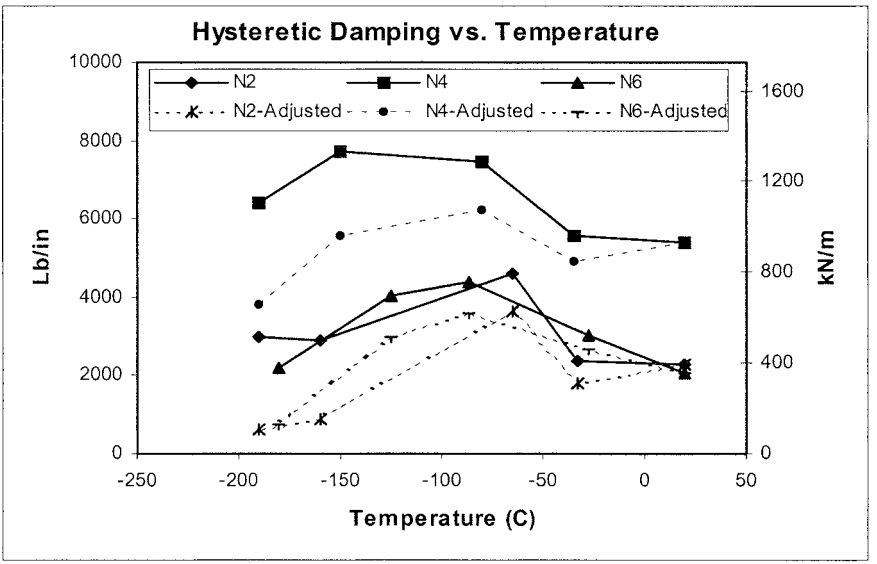

Figure 10: Hysteretic Damping Coefficients before and after Subtracting Interference Fit Contribution.

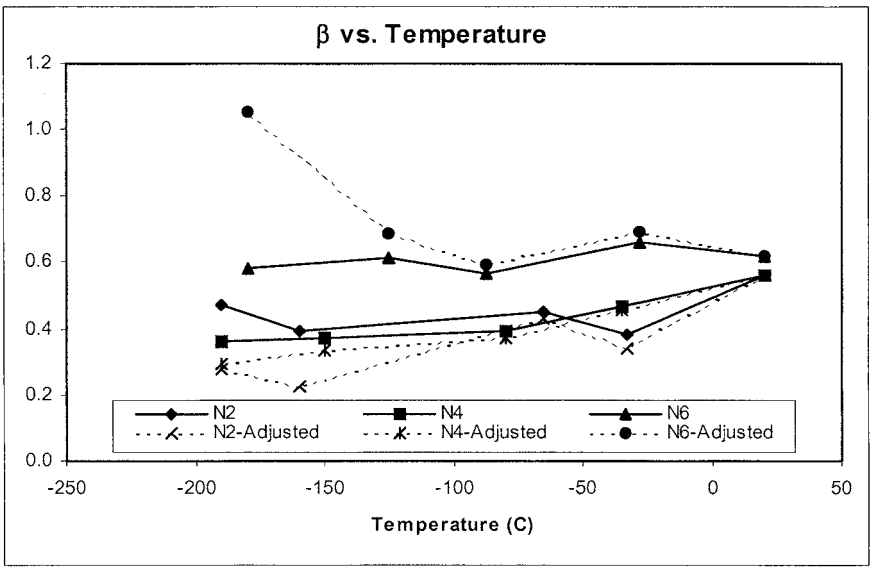

Figure 11: Loss Coefficients before and after Subtracting Interference Fit Contribution.

The contributions of increased interference to measured stiffness and damping values (K, C, H) were subtracted in the following manner. By taking the ambient coefficients (K_a, C_a, H_a) as references, the expression of the stiffness would be:

$$K = K_a + dK = K_a + (\partial K/\partial I)\cdot\ dI + (\partial K/\partial T)\cdot\ dT \tag{2}$$

Here, K and dK are functions of interference and temperature only since other factors were not varied in these tests. The last two terms in this equation are the change of stiffness due to interference (dK_I) and temperature (dK_T), respectively. The change of interference could be calculated from material expansion coefficient and measured temperature. Since we know the variation of stiffness with interference ($\partial K/\partial I$), as given by Al-Khateeb [1], we can then subtract the contribution of interference. From these calculated stiffness, damping and loss coefficient values, the dotted series in Figures 8 through 11 were plotted. Furthermore, by subtracting the measured ambient stiffness value, we obtain the change of stiffness due to temperature. This is given below, where expressions for damping are obtained in a manner similar to stiffness.

$$dK_T = K - K_a - (\partial K/\partial I)\cdot\ dI \tag{3}$$

$$dC_T = C - C_a - (\partial C/\partial I)\cdot\ dI \tag{4}$$

$$dH_T = H - H_a - (\partial H/\partial I)\cdot\ dI \tag{5}$$

Values calculated from the above equations are plotted in Figures 12 through 14. The resulting temperature-stiffness/damping correlations derived from these plots are summarized in Table 3. T_c in this table represents the calculated critical temperature at which reduction of temperature causes the parameter to become negative. This is basically when the coefficient (K, C, or H) becomes less than the measured ambient value. Critical temperatures are useful indicators when selecting wire mesh elements for applications with variable temperature.

To check the validity and usefulness of these relationships, we use them to calculate 'predicted' stiffness and damping values for the test results from Ertas et al. [4] shown in Table 2. The predicted values are calculated by summing the measured ambient coefficient, the change due to increased interference, and the change due to temperature. A comparison of the measured and predicted (calculated) values is given in Table 4.

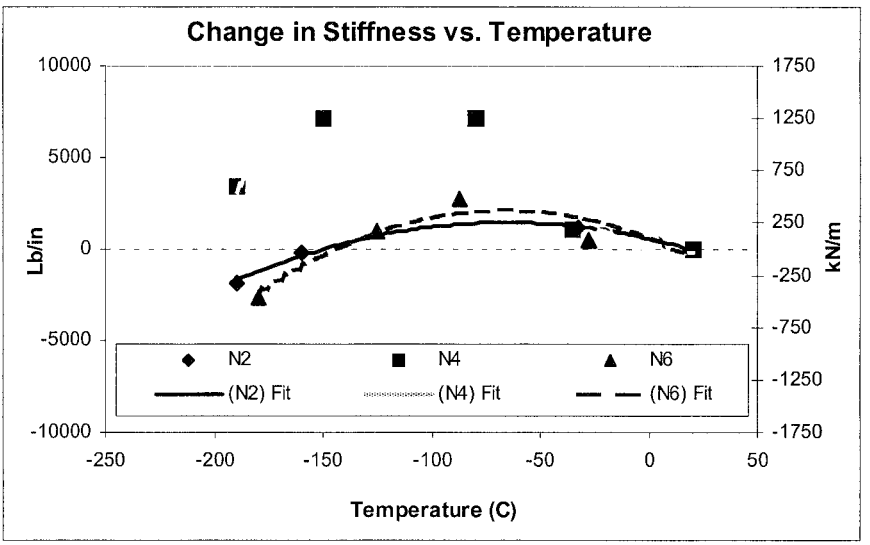

Figure 12: Change in Stiffness Due to Temperature.

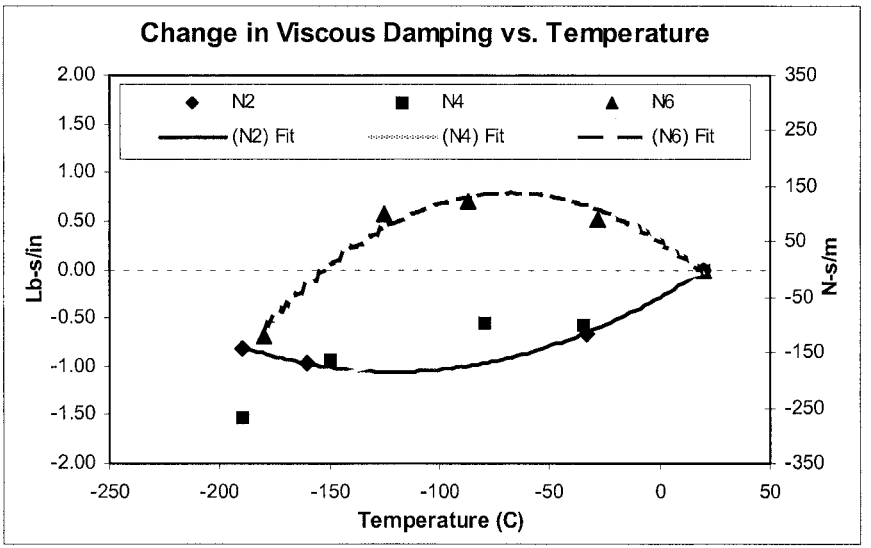

Figure 13: Change in Damping (Viscous) Due to Temperature.

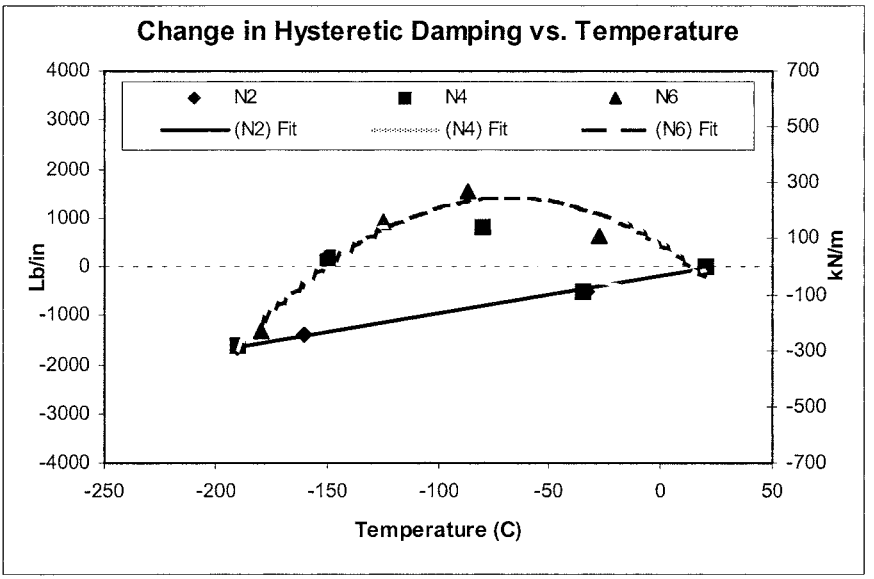

Figure 14: Change in Damping (Hysteretic) Due to Temperature.

Table 3: Correlations for Change of Coefficients with Temperature (T °C).

Wire Mesh	Parameter	Expression	Units	R^2	T_c (°C)
N2	$dK_T =$	$-0.0360\,\mathbf{T}^2 - 4.7280\,\mathbf{T} + 100.14$	kN/m	0.9902	-150
	$dC_T =$	$0.0088\,\mathbf{T}^2 + 2.2415\,\mathbf{T} - 49.646$	N-s/m	0.999	Ambient
	$dH_T =$	$1.3501\,\mathbf{T} - 33.486$	kN/m	0.9976	25
N4	$dK_T =$	$0.001\,\mathbf{T}^3 + 0.1698\,\mathbf{T}^2 - 5.5561\,\mathbf{T} - 2.7439$	kN/m	0.9269	-204
	$dC_T =$	$1.1208\,\mathbf{T} - 28.632$	N-s/m	0.9156	26
	$dH_T =$	$4E\text{-}04\,\mathbf{T}^3 + 0.0670\,\mathbf{T}^2 + 1.2466\,\mathbf{T} - 64.988$	kN/m	0.9264	-162
N6	$dK_T =$	$-0.0616\,\mathbf{T}^2 - 8.1157\,\mathbf{T} + 104.59$	kN/m	0.8652	-144
	$dC_T =$	$-0.0175\,\mathbf{T}^2 - 2.6092\,\mathbf{T} + 50.049$	N-s/m	0.9672	-166
	$dH_T =$	$-0.0365\,\mathbf{T}^2 - 4.9672\,\mathbf{T} + 77.362$	kN/m	0.9284	-150

Table 4: Comparison of Measured and Calculated Coefficients.

	Measured					Calculated			Percentage Difference			
Wire Mesh	T °C	K kN/m	C N-s/m	H kN/m	dI mm	K kN/m	C N-s/m	H kN/m	δK %	δC %	δH %	δβ %
N2	-175	1676	506.1	584	0.201	1675	523.1	658	-0.1	0.5	13	13
N4	-105	3761	798.5	1488	0.129	3521	600.0	1241	-6	-25	-16	-11
N4	-165	3144	584.3	967	0.191	3407	602.9	1189	8	3	23	13
N6	-155	1184	619.3	627	0.180	1100	632.3	616	-7	2	-2	6
N6 *	-190	2226	811.4	1170	0.217	1430	636.4	662	-36	-22	-43	-12
Average Absolute Difference									12	10	19	11

* *N6 Tested with a High Ambient Interference Fit of 0.559 mm (0.022 in).*

5 Discussion

The results show significant dependence on temperature, as expected of material behaviour. All the tested elements showed an increase in stiffness with temperature between ambient and critical temperatures (column Tc in Table 3). For viscous damping, only the copper mesh element (N6) increased in damping from ambient to the critical temperature. Similar behaviour is observed for the hysteretic damping, although the low-density steel mesh (N4) showed some increase along with its rising stiffness. N6, in particular, had almost parallel behaviour of its coefficients with temperature. Moreover, its Tc values are near to each other and far below ambient. This makes copper mesh more favourable for cryogenic turbomachinery applications. Reduction of coefficients below Tc may be offset by increasing the ambient interference fit, hence 'starting' with higher coefficient values.

The combination of efforts in modelling interference effects, from Al-Khateeb [1], and temperature effects from this study were very fruitful as can be seen from the results in Table 4. Overall, the differences between measured and modelled coefficients were reasonably low, considering that this is the first effort on modelling wire mesh dynamic coefficient variation with temperature. It is especially pleasant that the viscous damping was either accurately estimated or underestimated. This is significant since the predicted value would be a guaranteed minimum when the designed wire mesh element is put in service.

6 Conclusion

The understanding of temperature effects is essential for proper modelling and prediction of wire mesh coefficients when designing wire mesh bearing dampers. In conclusion, wire mesh dampers offer a feasible solution as bearing vibration dampers at cryogenic temperatures. Their usefulness at cryogenic temperatures was investigated and confirmed in this research. Design flexibility, low cost, requiring no lubrication, cooling, or auxiliary systems are all attributes of wire mesh that combine to its performance to produce a superior bearing damper for cryogenic applications. Of the three types of wire mesh tested in this study, copper wire mesh performed best. It demonstrated more linear behaviour, which is advantageous in modelling and prediction. Copper wire mesh is also more favourable form a rotordynamic perspective since it had lower stiffness and relatively high damping compared to other tested wire mesh.

Acknowledgment

The authors would like to acknowledge the support of METEX Corp., Pratt & Whitney, Lockheed Martin Astronautics, and Texas A&M University.

References

[1] Al-Khateeb, E.M., *Design, Modeling and Experimental Investigation of Wire Mesh Vibration Dampers*, Ph.D. Dissertation, Texas A&M University, 2002.

[2] Zarzour, Mark, and Vance, J.M., Experimental Evaluation of a Metal Mesh Bearing Damper, *ASME Journal of Engineering for Gas Turbines and Power*, April 2000.

[3] Al-Khateeb, E.M., and Vance, J.M., Experimental Evaluation of a Metal Mesh Bearing Damper in Parallel with a Structural Support. ASME Paper 2001-GT-0247, *Proceedings of the ASME Turbo Expo*, New Orleans, 2001.

[4] Ertas, B.H., Al-Khateeb, E.M., and Vance, J.M., Cryogenic Temperature Effects On Metal Mesh Dampers And Liquid Hydrogen Turbopump Rotordynamics. AIAA Paper 2002-4164, *Proceedings of the 38th AIAA/ASME/SAE/ASEE Joint Propulsion Conference and Exhibit*, Indianplois, 2002.

[5] Okayasu, A., Ohta, T., Azuma, T., Fujita, T., and Aoki, H., Vibration Problems in the LE-7 Liquid Hydrogen Turbopump. *Proceedings of the 26th AIAA Joint Propulsion Conference*, pp.1-5, 1990.

[6] Childs, D.W., The Space Shuttle Main Engine High-Pressure Fuel Turbopump Rotordynamic Instability Problem. *ASME Journal of Engineering for Power*, **100(1)**, pp. 48-57, 1978.